International Journal of Concrete Structures and Materials

RESEARCH Open Access

Variation of the Hydraulic Conductivity and the Mechanical Characteristics of Plastic Concrete with Time

Ali Basha and Walid Mansour*

Abstract

Sand-bentonite-cement are commonly used as cut-off walls to isolate polluted soils or in ground improvement technologies and as retaining structures as secant pile wall. In this research, a laboratory program consisted from 105 sample were prepared and tested between different tests, such as hydraulic conductivity, porosity, and compressive strength to monitor the mechanical behavior of sand-bentonite-cement at different ages. Based on the experimental relationships between hydraulic conductivity coefficient and samples age; there were reduction due to added bentonite to mixture reach about 35.0% at 7 days. Moreover, the average reduction in the compressive strength of plastic concrete samples with bentonite was lower by average range about 51.0% than the compressive strength of plastic concrete samples without bentonite at 7 days. In this study, proposed formulas were derived to estimate the splitting tensile strength based on the compressive strength and the hydraulic conductivity in terms of the bentonite/cement ratio and testing age. The predicted values showed well agreement with the experimental records for samples of sand-bentonite-cement mixtures where the standard deviation and coefficient of variation were 0.02, and 0.94%, respectively.

Keywords Plastic concrete, Secant pile, Hydraulic conductivity, Compressive strength, Tensile strength

1 Introduction

Secant pile walls have been widely used as a cost-effective retaining wall technique in deep excavation sites especially in the coastal cities and the metro lines. It is used mainly to minimize the lateral deformation and to control groundwater flow toward the excavation site. In the recent years, the interest in plastic concrete incorporating bentonite which is impervious material has increased especially in the secant piles. The need to decrease the compressive strength and the shear strength of plastic concrete becomes a main requirement in constructing the geotechnical project especially in the secant pile walls as stated by El-Nimr et al. (2022).

Water tightening and seepage control are important factors to consider when designing and building secant pile walls. Plastic concrete is made up of aggregate particles, cement, water, and bentonite that are combined at a high water-to-cement ratio to create a ductile construction mixes (Hinchberger et al., 2010; Liu et al., 2011; Xiong et al., 2011). Plastic concrete walls mainly act as a barrier to prevent or reduce groundwater flow (Chandrappa & Biligiri, 2016; Huang et al., 2010; Sandoval et al., 2017; Wu et al., 2016). Plastic concrete in such applications must have a low elastic modulus with respect to the foundation (Bagheri et al., 2008). Plastic concrete has a very high water-to-binder ratio in order to meet the minimal elastic modulus demands (Alós Shepherd et al., 2020; Barnhouse & Srubar, 2016; Gao et al., 2009; Wang et al., 2011). Additional prerequisites

Journal information: ISSN 1976-0485 / eISSN 2234-1315

*Correspondence:
Walid Mansour
waled_mansour@eng.kfs.edu.eg
Department of Civil Engineering, Faculty of Engineering, Kafrelsheikh University, Kafrelsheikh 33511, Egypt

for plastic concrete include sufficient strength to resist the design loads and low enough permeability to control seepage and reduce groundwater flow (Fadaie et al., 2019; Flessati et al., 2021; Guo & Zhu, 2008; Iravanian & Bilsel, 2016; Royal et al., 2017; Ziccarelli & Valore, 2018).

Zhang et al. (2013) experimentally examined the mechanical properties of plastic concrete containing bentonite. It seems using higher water-to-binder ratio and bentonite dosage can be beneficial in improving the resistance against deformation of plastic concrete cut-off walls.

Sandoval et al. (2020) performed an experimental program to test and characterize the hydraulic behavior variation of pervious plastic concrete with natural aggregates and recycled aggregates due to clogging. Plastic concrete's hydraulic conductivity is reduced not only due to the porosity of plastic concrete but also by the particle size distribution of sediments, and the hydraulic conductivity of plastic concrete with natural aggregates is more affected by the addition of sediments than plastic concrete with recycled aggregates.

Previous researchers (Bhutta et al., 2012; Castro et al., 2009; Ibrahim et al., 2014; Kevern et al., 2009; Maguesvari & Narasimha, 2013; Neithalath et al., 2010; Tho-in et al., 2012) have extensively studied the relationship between permeability and porosity in plastic concrete. Different responses to these two parameters were recorded, either as an exponential or linear trend. Table 1 shows that the results of the correlation between permeability and porosity found in the literature differ significantly. As a result, more research is required to investigate the relationship between permeability in terms of hydraulic conductivity and porosity, which is one of the current research goals.

2 Strategy of the Study

Sand-bentonite-cement mixtures are commonly used as a barrier material, so the hydraulic conductivity and the mechanical properties are often required for the structural and geotechnical design of the barrier, such as a secant pile wall. During groundwater transport through the soil and crossing the secant pile walls, different types of soluble matter, whether organic or inorganic, are transported and can lead to a decrease in the hydraulic conductivity and change the mechanical properties. The main purpose of the current study is to experimentally investigate the characterization of mechanical and hydraulic conductivity properties of secant pile material under different key parameters, such as water-to-cement ratio, bentonite-to-cement ratio, cement content, and sample age. The effect of these parameters on the mechanical properties, such as compressive strength, the split tensile strength, and the hydraulic conductivity of all mixtures, was measured. Based on the knowledge gaps previously presented, this study aims to investigate the variation of hydraulic conductivity of secant pile wall material and the mechanical properties with time. A laboratory program was designed to achieve the proposed objective, as shown in Fig. 1.

3 Experimental Program

3.1 Materials

3.1.1 Cement

In the current investigation, ordinary Portland cement (OPC), CEM II, manufactured by Assuit-Plant was used during casting of plain concrete mixtures. Chemical components of the used cement according to the manufacturer are listed in Table 2, while physical characteristics, experimentally recorded, such as specific gravity, fineness, as well as compressive strengths at various ages, are shown in Table 3.

Table 1 The correlations for hydraulic conductivity

Reference	Correlation	year
Castro et al. (2009)	$K = 0.840*e^{0.09P}$	2009
Kevern et al. (2009)	$K = 19.17*e^{0.14P}$	2009
Neithalath et al. (2010)	$K = (0.40*e^{11.3P})10^{-10}$	2010
Tho-in et al. (2012)	$K = 0.0447*e^{0.1388P}$	2011
Bhutta et al. (2012)	K = 0.2927*P—4.97	2011
Maguesvari and Narasimha (2013)	$K = 0.067*e^{7.246P}$	2013
Ibrahim et al. (2014)	K = 0.8074 + 0.0109*Cement content + 0.2714* water/cement + 0.0707*water + 0.0015*Aggregate (4.50 mm (+ 0.0024*Aggregate (9.50 mm) + 0.0019*Aggregate (19.5 mm)	2014

where *K* is the hydraulic conductivity coefficient and *P* is the porosity

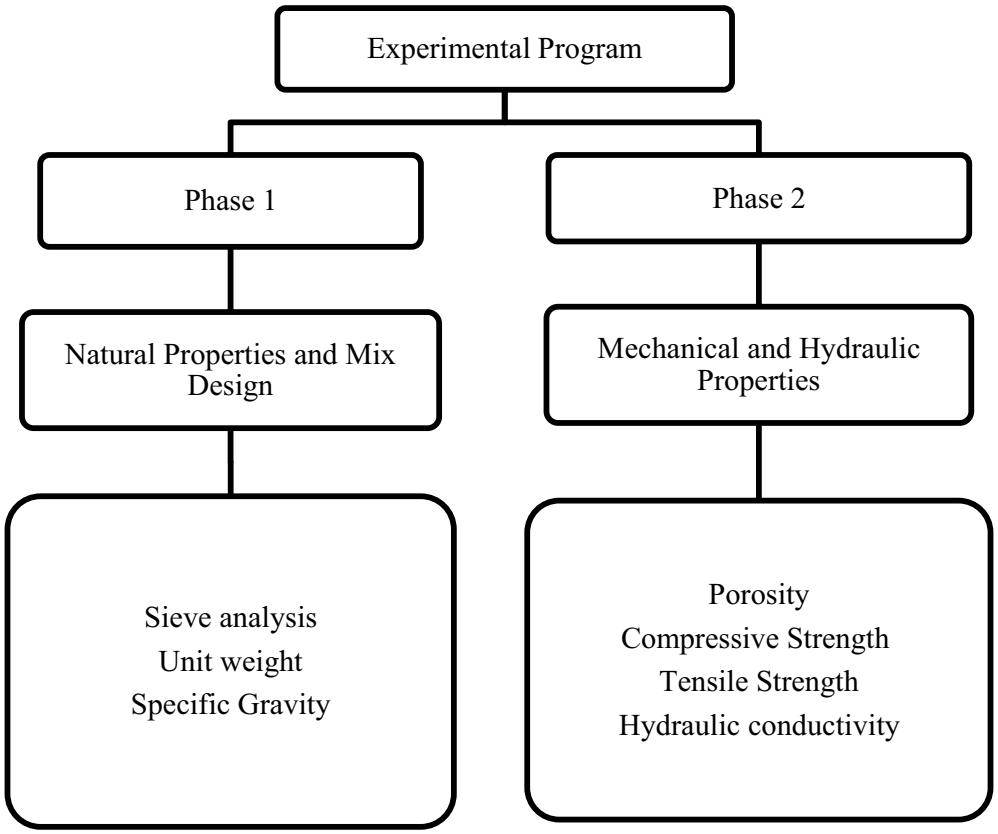

Fig. 1 The experimental program

Table 2 The chemical composition of the used cement

Component	SiO2	Al2O3	Fe2O3	CaO	MgO	SO3	Na2O	K2O
Proportion %	16.90	4.70	5.44	34.66	1.74	1.53	0.77	0.41

Table 3 Results of the physical characteristics of the used cement

Specific Gravity	Fineness, (Blaine test) cm^2/gm	Compressive strength MPa		
		3 days	7 days	28 days
3.15	3200	18	26	37

3.1.2 Fine and Coarse Aggregates

In the current experimental program, clean silica sand with maximum grain size of approximately 5 mm was used as fine aggregate, while crushed basalt with maximum grain size of approximately 20 mm was utilized as coarse aggregate. A sieve analysis test was performed on both fine and coarse aggregates and the recorded grain size distribution is depicted in Fig. 2. Additionally, the physical properties of the used fine and coarse aggregates are experimentally measured and summarized in Table 4.

3.1.3 Bentonite

The bentonite has been utilized in this paper to facilitate the cut-off inside the secant pile walls in addition to reducing the conductivity of the plain concrete. The chemical components and physical characteristics of the bentonite are shown in Tables 5 and 6, respectively.

3.1.4 Mixing Water

River water (tab water) was used for mixing and curing the concrete specimens as well as for performing the hydraulic conductivity tests. The chemical and physical properties of the used water are PH = 7.70, temperature = 22 °C, total dissolved soluble (TDS) = 350 mg/l, sulfates = 60 mg/l, and chlorides = 4.5 mg/l.

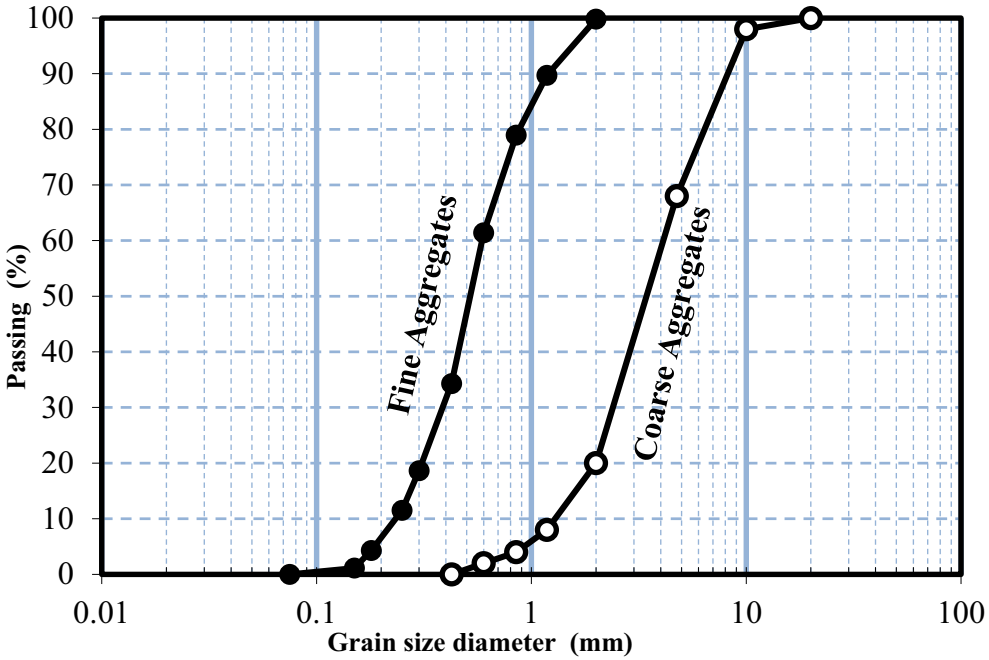

Fig. 2 Fine and coarse aggregates grain size distribution

Table 4 Physical properties of the used fine and coarse aggregates

Property	Fine Aggregate (Sand)	Coarse Aggregate (Crushed basalt)
Effective grain size, D_{10} (mm)	0.23	1.20
Average grain size, D_{30} (mm)	0.38	2.50
Average grain size, D_{60} (mm)	0.60	4.20
Uniformity coefficient, C_u	2.60	3.50
Coefficient of curvature, C_c	1.04	1.24
Maximum dry unit weight, γ_d max (kN/m^3)	18.48	19.68
Minimum dry unit weight, γ_d min (kN/m^3)	16.77	17.07
Maximum void ratio, e_{max}	0.571	0.571
Minimum void ratio, e_{min}	0.399	0.399
Specific gravity, G_s	2.65	2.67
Classification (USCS, ASTM)	Poorly graded sand (SP)	Poorly graded gravel (GP)

Table 5 The chemical components of the used bentonite

Components	SiO2	Al2O3	Fe2O3	CaO	MgO	Na2O	K2O
Proportion %	59.90	16.51	5.31	4.55	2.41	3.54	1.08

3.2 Plastic Concrete Mixtures Design

The experimental program consisted of five different mixtures. The first mixture was considered as the control group and was cast without bentonite. On the other hand, the other four groups were cast using different ratios of bentonite as listed in Table 7. The mixing process for the control group was as follows: the sand and half amount of water were added into the mixer and mixed for two minutes. In the next step, the cement content and the quarter amount of water were added into the mixer and mixed

Table 6 The physical properties of the used bentonite

Specific Gravity	Ph (5% Con.)	Moisture Content %	Dry Screen Analysis Passing No 100 %	Wet Screen Analysis Passing No 200 %	Sand Content %	Liquid Limit %	Plastic Limit %	Plasticity Index %
2.60	10	10	99	98.5	0.20	450	30	420

Table 7 Mixture proportions for plastic concrete (one batch)

Group	Weight				Ratio		
	Cement (kg)	Sand (kg)	Bentonite (kg)	Water (kg)	B/S	B/C	W/C
I	30	105	–	15.00	–	–	0.50
II	30	105	5.25	35.00	0.050	0.175	1.10
III	30	105	7.35	35.00	0.0750	0.2625	1.10
IV	30	105	10.5	35.00	0.100	0.350	1.10
V	30	105	13.125	35.00	0.125	0.4375	1.10

B/S= Bentonite/Sand

B/C= Bentonite/Cement

W/C= Water/Cement

for additional two minutes. Finally, the rest of water was added into the mixture and mixed for extra two minutes to reach a homogeneous combination as stated by Sandoval et al. (2020). For the other four groups, the amount of bentonite was added along with the amount of cement.

Forty-five cylinders of 100 mm in diameter and 300 mm in height were prepared and cast to perform the splitting tensile test while fifteen cylindrical specimens of 100 mm in diameter and 200 mm in height were manufactured for the hydraulic conductivity test. Additionally, a total of forty-five cubes of 150 mm × 150 mm × 150 mm were compiled for the compressive test. Both the cylindrical and cubic specimens were demolded after 48 h and cured in water until the testing age (7, 14, 21, 28, and 120 days).

3.3 Test Methods

3.3.1 Cubes

To investigate the variation of the compressive strength with time, the cubic specimens previously prepared were tested at 7, 14, 21, 28, and 120 days based on the specifications of the Egyptian code ECP-203 (ECP, 2017). The NTROLS testing machine with total capacity of 1000 kN and loading speed of 200 ± 15 N/second was used to perform the test. Moreover, a manual displacement gauge of 30 mm length was utilized to record the settlement/shortening of the cubes during the test as shown in Fig. 3a. At the end of the test, the compressive stresses and the corresponding strains could be easily estimated using Eqs. (1) and (2), respectively.

$$\sigma_c = \frac{P}{A_c}, \tag{1}$$

$$\varepsilon_c = \frac{\Delta_c}{L_c}, \tag{2}$$

where σ_c is the calculated stress in compression (MPa), P is the implemented load (N), A_c is the cube's area (mm^2), ε_c is the compressive strain, Δ_c is the shortening/settlement (mm), and L_c is the cube's length (mm).

3.3.2 Cylinders

The splitting tensile strength of both the control and the plastic concrete specimens is measured according to the Brazilian test in accordance with the ASTM C496 (ASTM-C496. Splitting tensile strength of cylindrical concrete", 1996) at 7, 14, 21, 28, and 120 days. The NTROLS testing machine is used as depicted in Fig. 3(b) and the splitting tensile stress of the cylindrical specimens is calculated by using Eq. (3):

$$\sigma_t = \frac{2P}{\pi LD}, \tag{3}$$

where σ_t is the tensile stress (MPa), P is the failure load in the Brazilian test (N), L is the specimen's length (mm), and D is the specimen's diameter (mm).

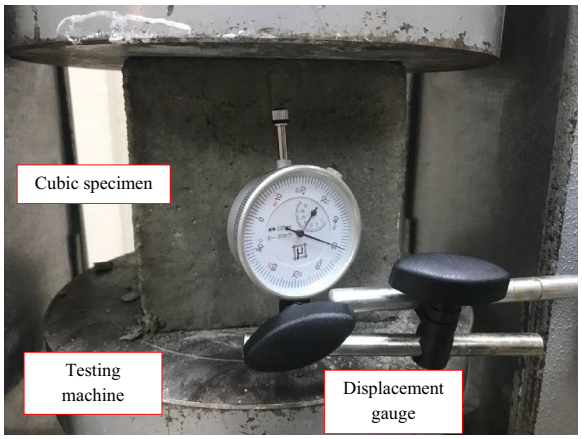

(a)

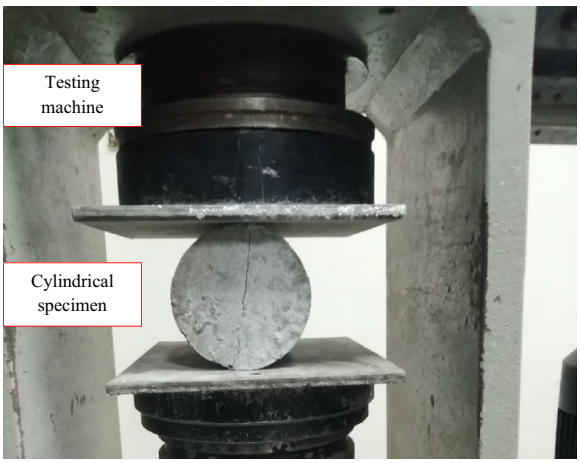

(b)

Fig. 3 Test set-up **a** compression and **b** splitting tensile

3.3.3 Specimens' Porosity

The porosity of the cylindrical specimens was calculated as the difference of the submerged weight in water and the air-dried for 24 h weight of the cylinder specimens divided by the volume, Eq. (4), as specified by Park and Tia (2004).

$$P = \left[1 - \left(\frac{w_1 - w_2}{v_1 \rho_w}\right)\right], \tag{4}$$

where P is the total porosity as percentage (%), w_1 is the air-dried for 24 h weight, w_2 is submerged weight in the water,v_1 is the volume of the cylinder, and ρ_w is the water density.

3.3.4 Failing Head Test Set-up

As previously reported, one of the main objectives from the utilization of bentonite is to control the seepage along the secant pile wall. To the authors' best knowledge, till now there is no specific standard test to determine the hydraulic conductivity of plastic concrete. As a result, the falling head test was carried out in the laboratory on the basis of Zhang et al., (2013, Sandoval et al. (2020, and Xu et al. (2016) in order to investigate the hydraulic conductivity of the plastic concrete. An end valve has been installed at the apparatus to get rid of the water that pass through the cylindrical specimen as shown in Fig. 4. Once the falling head system is completed, the specimen is saturated with a water column height of 25 cm. In the next step, the valve is opened and the time required to decrease the water column height from 25 to 5 cm was observed. Hence, the hydraulic conductivity of the specimens is estimated using Eq. (5):

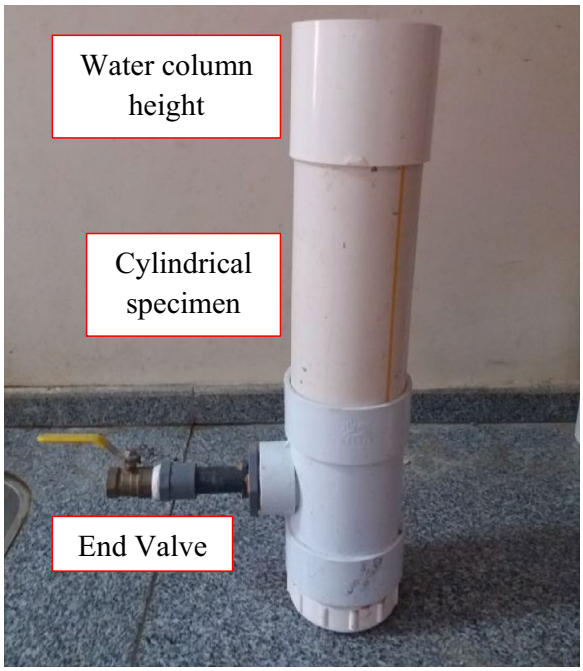

Fig. 4 Falling head test set-up

$$\mathrm{k} = \frac{L}{t} \times \ln \frac{h_1}{h_2}, \tag{5}$$

where k is hydraulic conductivity (m/s), L is the specimen's length (m),t is the time required to reduce the water height from h_1 to h_2, h_1 is the initial water column height = 25 cm, and h_2 is the final water column height = 5 cm.

4 Results and Discussions

4.1 Compressive Strength

The compressive strengths of control and plastic concretes at various ages are shown in Table 8. Generally,

Table 8 Results of compressive strength at different ages

Group	7 days	% decrease	14 days	% decrease	Compressive Strength (MPa)					% decrease
					21 days	% decrease	28 days	% decrease	120 days	
I	7.09	–	11.27	–	11.58	–	12.09	–	12.22	–
II	4.13	42	5.33	53	7.20	38	9.51	21	10.09	17
III	3.91	45	4.67	59	6.71	42	8.31	31	8.84	28
IV	3.9	45	4.52	60	5.33	54	6.84	43	7.02	43
V	2.02	72	3.29	71	3.78	67	4.00	67	4.44	64

the control specimens (without bentonite) had higher compressive strengths at all tested ages with respect to the plastic concrete mixtures (with bentonite). The compressive strength of control concrete at 7, 14, 21, 28, and 120 days was 7.09, 11.27, 11.58, 12.09, and 12.22 MPa, respectively. At the same testing age, as the bentonite content increased, the compressive strength of the plastic concrete decreased. It may be referred to that the high concentrations of bentonite surround the fine aggregate in addition to preventing the hydration of the total cement content. On the other hand, the testing age has a significant effect on the compressive strength. The reduction in compressive strength at 120 days remarkably enhanced compared to 7, 14, 21, and 28 days. At 7 days, the reduction in compressive strength of mix II with bentonite/sand ratio of 5%, mix III with bentonite/sand ratio of 7.5%, mix IV with bentonite/sand ratio of 10%, and mix V with bentonite/sand ratio of 12.5% was 42, 45, 45, and 72% compared to the control mix I. The compressive strength of all the plastic concrete mixtures at 14 days was enhanced, while the reduction in compressive strength compared to the control specimen was not improved. The reduction in compressive strength was in the range of 53–71% with respect to mix I. The same pattern was approximately noticed at 21 days. On the contrary, both the value and the reduction in the compressive strength were significantly enhanced at 28 and 120 days for mix II and III due to the existence of lower bentonite content. The compressive strength of mix II and III at 120 days only was 17 and 28% lower than the control mix I, while their counterparts' ratios at 7 days were 42 and 45%, respectively. On the other hand, the reduction in compressive strength for mix IV and V with high content of bentonite was not enhanced event at 120 days. The reduction in compressive strength for mix IV and V compared to mix I at 7 days was 45 and 72%, while the same rations at 120 days were 43 and 64%, respectively.

4.2 Compressive Strain

Fig. 5 shows the compressive stress–strain for the control and the plastic concretes at various ages. All specimens exhibited bi-linear behavior; a linear stage followed by a horizontal region. For the specimens tested at 7 days, the stiffness of the conventional concrete (the slope of the linear stage) was higher than the plastic concretes. Moreover, the control concrete developed higher strains at failure with respect to the plastic concrete. The compressive strain at failure for mix I, II, III, IV, and V was 1.65, 1.35, 1.35, 1.44, and 1.00%, respectively. As the testing age increased both the stiffness and the strain at failure were significantly improved. The stiffness of the plastic concrete remarkably enhanced as the testing age increased due to the increase of the compressive strain. The stiffness of the plastic concrete at 21, 28, and 120 days was approximately the same as well as the control concrete. Additionally, at 28 and 120 days, the strain of the plastic concrete increased compared to earlier ages and approximately reached a strain of 1.4%.

4.3 Splitting Tensile Strength

Table 9 displays the results of the splitting tensile tests at different ages. The deterioration mechanism observed in the compressive strength results due to the presence of the bentonite approximately repeated in case of the splitting tensile strength. On the other hand, the tensile strength results were not improved with the increase of the testing except for mix II with the lowest bentonite content. The tensile strength of the control mixes was 0.76, 0.94, 0.96, 0.97, and 0.98 MPa at 7, 14, 21, 28, and 120 days, respectively. For mix II, the reduction in the tensile strength was 50 and 57% compared to mix I at 7 and 14 days, respectively. As the testing age increased, the reduction in splitting strength of mix II remarkably enhanced. The splitting strength of mix II was 38, 20, and 15% lower than the control mixes at 21, 28, and 120 days, respectively. On the contrary, the reduction in the splitting strength of the other three mixtures III, IV, and V was kept constant despite the variation of the testing age. The reduction in splitting strength of mix III, IV, and V was in the range of 50–59%, 61–65%, and 68–72%, respectively.

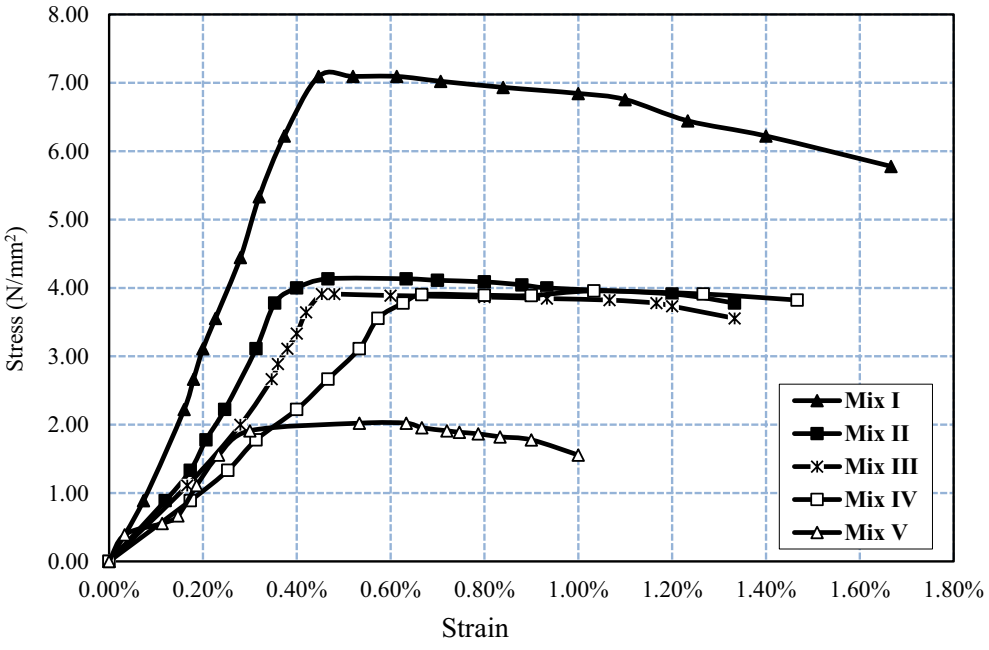

(a)

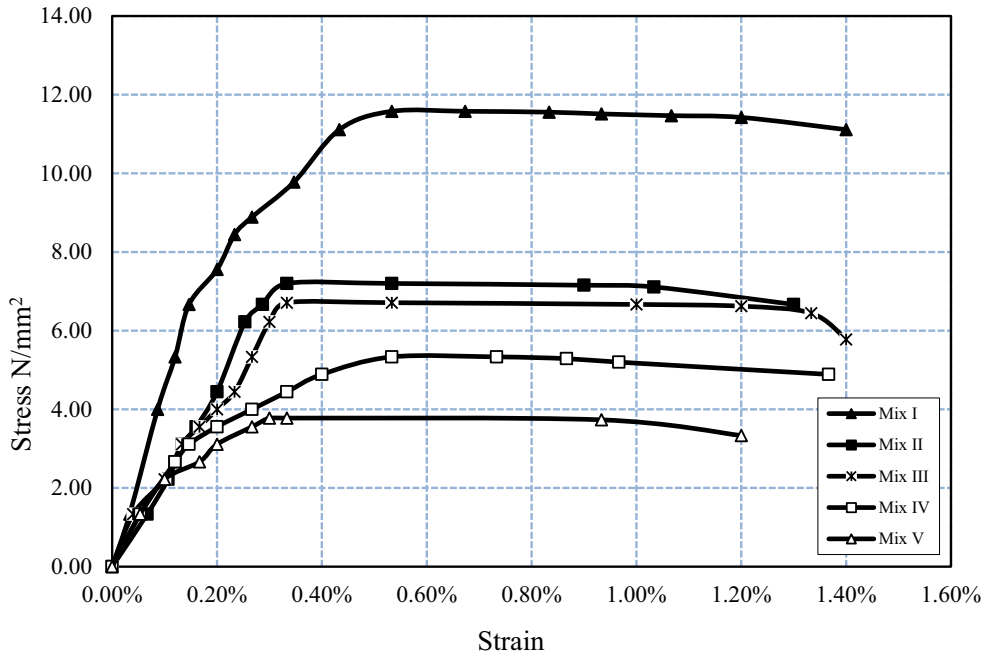

(b)

Fig. 5 Stress–strain curve for control and plastic concretes specimens for the curing periods of different ages **a** 7 days, **b** 21 days, **c** 28 days, and **d** 120 days

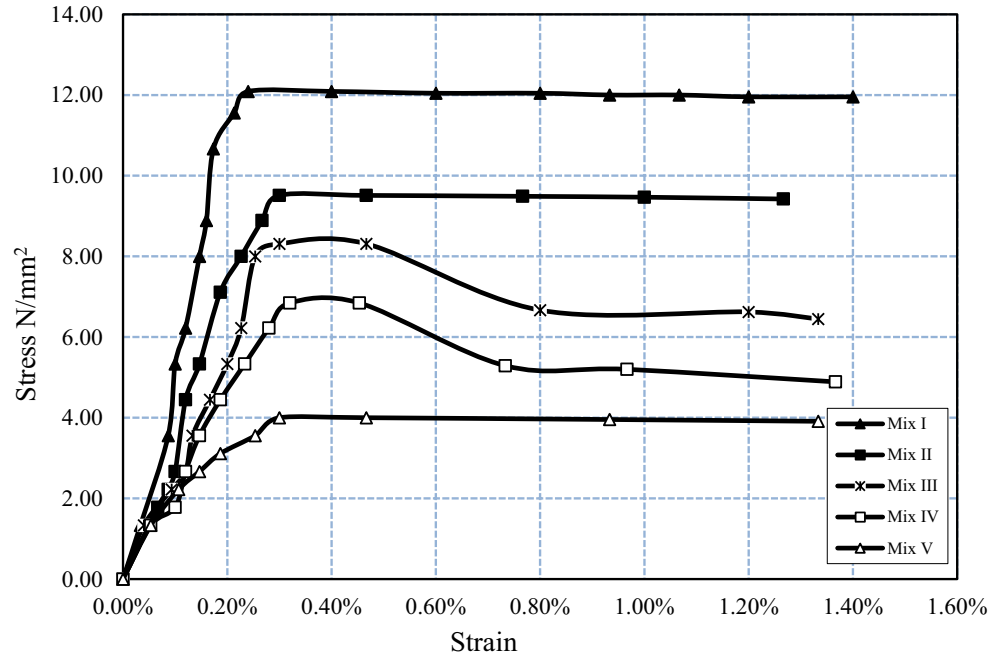

(c)

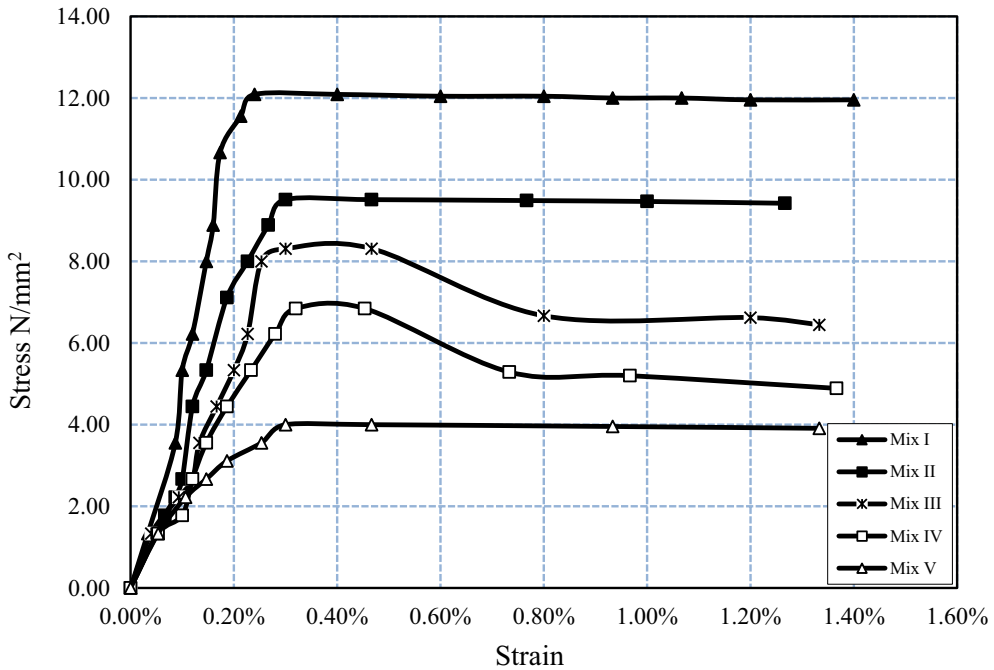

(d)

Fig. 5 continued

Table 9 Results of the splitting tensile strength tests

Group	7 days	% decrease	14 days	% decrease	Splitting Tensile Strength (MPa)					% decrease
					21 days	% decrease	28 days	% decrease	120 days	
I	0.76	–	0.94	–	0.96	–	0.97	–	0.98	–
II	0.38	50	0.40	57	0.59	38	0.77	20	0.83	15
III	0.35	54	0.39	59	0.42	56	0.45	53	0.49	50
IV	0.30	61	0.33	65	0.34	64	0.37	61	0.38	61
V	0.24	68	0.26	72	0.28	70	0.29	70	0.30	69

Table 10 Experimental splitting tensile strength of the control concrete versus the theoretical results calculated using the ECP-203

Group	Bentonite / Sand	Compressive strength (MPa)	Splitting Tensile Strength (MPa)		
		Experimental	Experimental (EXP)	Theoretical (THE)	THE / EXP
Control concrete	0	7.09	0.76	1.59	2.09
		11.27	0.94	2.01	2.13
		11.58	0.96	2.04	2.12
		12.09	0.97	2.08	2.14
		12.22	0.98	2.09	2.13
Average					2.12
Standard deviation					0.02
Coefficient of variation (COV)					0.94%

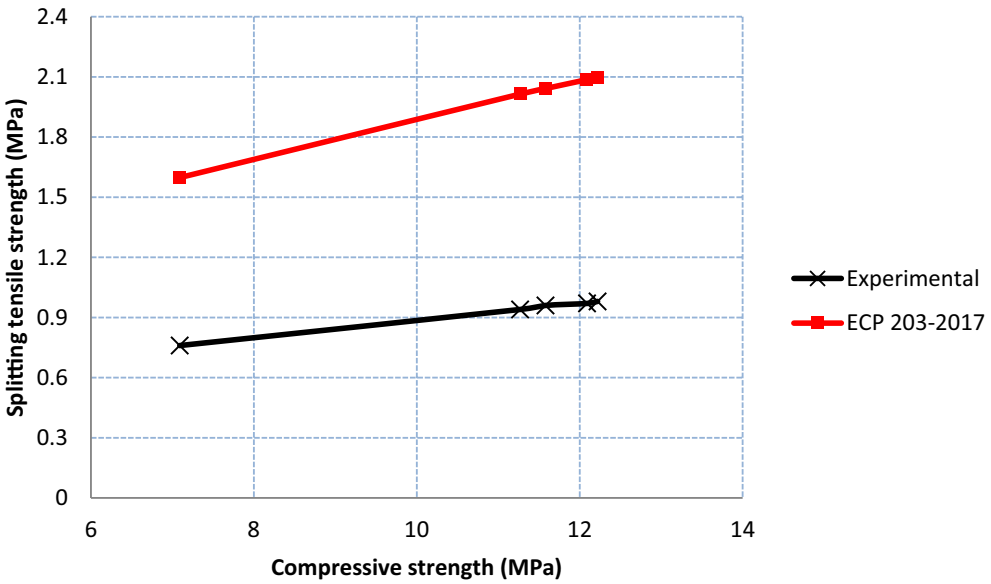

Fig. 6 Relationship between the experimental and the theoretical splitting tensile strength versus the experimental compressive strength for the control concrete

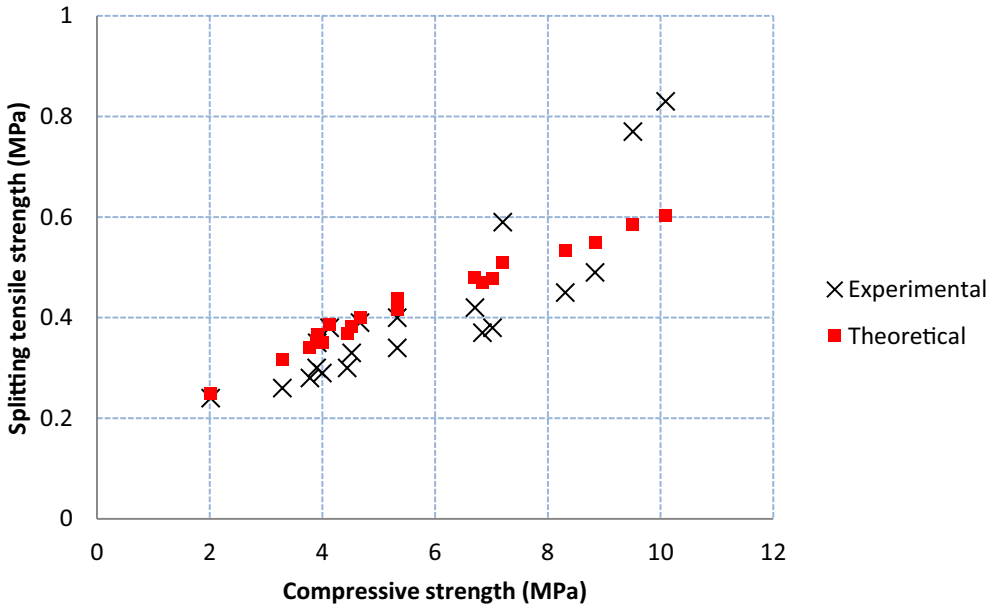

Fig. 7 Relationship between the experimental and the theoretical splitting tensile strength versus the experimental compressive strength for the plastic concrete

Table 11 Experimental splitting tensile strength of the plastic concrete versus the results of the predicted equation

Group	B/S	Compressive strength (MPa)	Splitting Tensile Strength (MPa)		
		Experimental	Experimental (EXP)	Theoretical (THE)	THE / EXP
Plastic concrete	0.05	4.13	0.38	0.38	1.00
		5.33	0.40	0.43	1.08
		7.20	0.59	0.50	0.85
		9.51	0.77	0.58	0.75
		10.09	0.83	0.60	0.72
	0.075	3.91	0.35	0.36	1.03
		4.67	0.39	0.39	1.00
		6.71	0.42	0.47	1.12
		8.31	0.45	0.53	1.18
		8.84	0.49	0.55	1.12
	0.10	3.90	0.30	0.35	1.17
		4.52	0.33	0.38	1.15
		5.33	0.34	0.41	1.21
		6.84	0.37	0.47	1.27
		7.02	0.38	0.47	1.24
	0.125	2.02	0.24	0.24	1.00
		3.29	0.26	0.31	1.19
		3.78	0.28	0.34	1.21
		4.00	0.29	0.35	1.21
		4.44	0.30	0.36	1.20
Average					1.08
Standard deviation					0.16
Coefficient of variation (COV)					15%

4.4 Relationship Between the Splitting Tensile Strength and the Compressive Strength

In this section, the splitting tensile strength of the control concrete is estimated based on the ECP-203 (ECP Housing & Building National Research Center, Egyptian Code for Designing & Constructing Reinforced Concrete Structures, 2017) code guidelines and the recommendation of Mansour and Fayed (2021); Sakr et al., (2018); and Mansour et al., (2022) using Eq. (6) considering only the concrete compressive strength and compared with the experimental records as shown in Table 10. Results shown in Fig. 6 revealed that the Egyptian code overestimating the splitting tensile strength on the concrete. Ratios between the predicted and the experimental values ranged from 2.09 to 2.14 with average value, standard deviation, and coefficient of variation of 2.12, 0.02, and 0.94%, respectively.

$$\sigma_t = 0.6\sqrt{\sigma_c}. \tag{6}$$

Additionally, the splitting tensile strength of the plastic concrete is theoretically predicted using the proposed formula in Eq. (7). The suggested equation considers both the bentonite/sand ratio $\left(\frac{B}{S}\right)$ as well as the compressive strength of the plastic concrete. Fig. 7 shows that the predicted results well agree with the experimental records. Also, the statistical findings in Table 11 display that the average value between the theoretical/experimental ratios is 1.08, while the standard deviation and the coefficient of variation are 0.16 and 15%, respectively.

$$\sigma_t = 0.2\left(1 - \frac{B}{S}\right)\sqrt{\sigma_c}. \tag{7}$$

Table 12 Porosity test results (%)

Mix Group	I	II	III	IV	V
7 days	22	20	17	17	15
14 days	22	20	17	17	14
21 days	20	18	16	15	14
28 days	18	18	15	15	13
120 days	18	17	14	15	12
Average	20	18.6	15.8	15.8	13.6
Standard deviation	2	1.3	1.30	1.1	1.14
Coefficient of variation (%)	10	6.7	6.5	5.5	5.7

4.5 Porosity

Fig. 8 displays the porosity results of the tested mixtures at different ages. For the same mixture, as the testing age increased, the porosity was significantly reduced. The reduction in porosity between 120 and 7 days was 18.2%, 10%, 17.6%, 11.8%, and 20% for mix I, mix II, mix III, mix IV, and mix V, respectively. Additionally, the high concentration of bentonite within the mixture remarkably

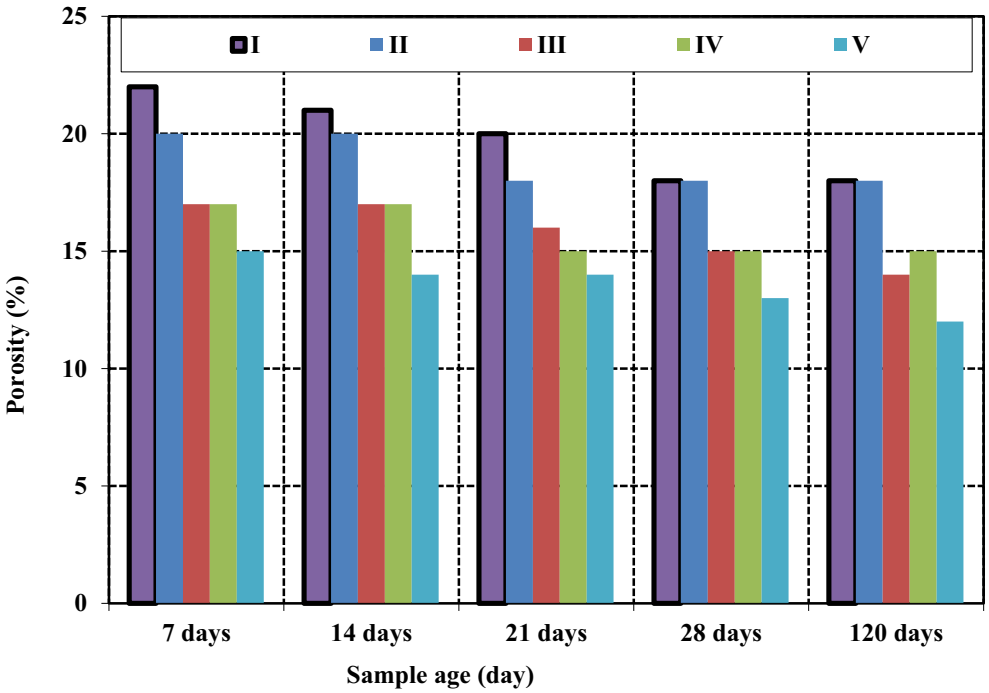

Fig. 8 Change of the porosity with time

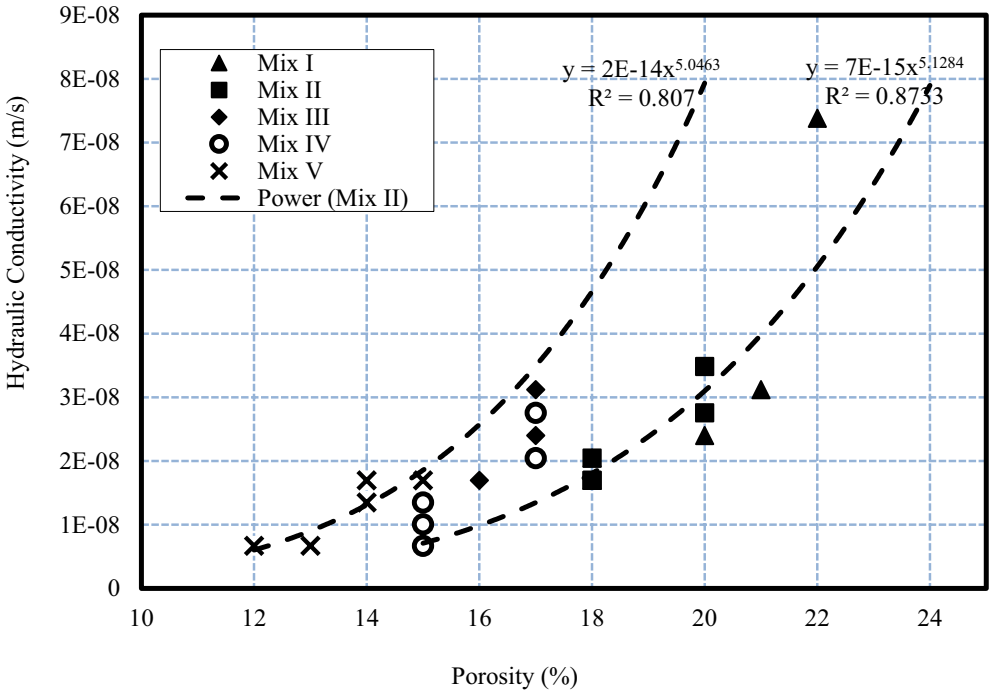

Fig. 9 Change of hydraulic conductivity with the porosity

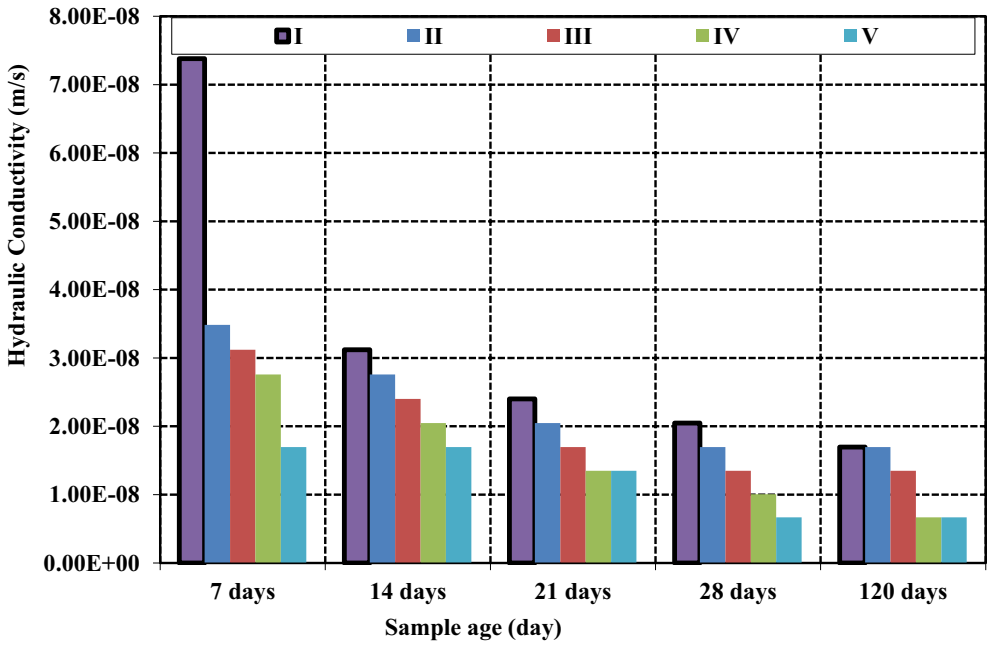

Fig. 10 Change of hydraulic conductivity with time

improved the porosity with respect to the control mixture. The reduction in porosity for mix II, mix III, mix IV, and mix V was 9.1%, 22.7%, 22.7%, and 31.8% at 7 days, while their counterparts value at 120 days were 5.6%, 22.2%, 16.7%, and 33.3%, respectively, as shown in Table 12.

Fig. 9 shows the experimental records for the falling head permeability test (hydraulic conductivity) versus the

Table 13 Falling head permeability test results (m/s)

Mix Group	I	II	III	IV	V
7 days	7.38E−08	3.48E−08	3.11E−08	2.75E−08	1.69E−08
14 days	3.11E−08	2.75E−08	2.40E−08	2.04E−08	1.69E−08
21 days	2.40E−08	2.04E−08	1.69E−08	1.35E−08	1.35E−08
28 days	2.04E−08	1.69E−08	1.35E−08	1.01E−08	6.68E−09
120 days	1.69E−08	1.69E−08	1.35E−08	6.68E−09	6.68E−09
Average	3.32E−08	2.33E−08	1.98E−08	1.56E−08	1.21E−08
Standard deviation	2.32E−08	7.74E−09	7.66E−09	8.39E−09	5.19E−09
Coefficient of variation (%)	69.86	33.14	38.63	53.57	42.73

experimental records of the porosity for different mixes. Based on the experimental result; the following two exponential correlations between hydraulic conductivity coefficient and the porosity represent the upper and lower boundary with regression coefficient R^2 of 0.807 and 0.8733, respectively, as follows:

The exponential correlations for upper limit

$$K = 2 \times 10^{-14} P^{5.046}. \quad (8)$$

The exponential correlations for lower limit

$$K = 7 \times 10^{-15} P^{5.1284}. \quad (9)$$

4.6 Hydraulic Conductivity

Fig. 10 shows the experimental records for the falling head permeability test (hydraulic conductivity) versus the sample age, while Table 13 demonstrates the statistical data analysis. It can be observed that the hydraulic conductivity of both control and plastic concretes gradually decreased with the increase of the testing age. On one hand, for the control group, the hydraulic conductivity at 7, 14, 21, 28, and 120 days was 7.38E−08, 3.11E−08, 2.40E−08, 2.04E−08, and 1.69E−08 m/s, respectively, accompanied with average value, standard deviation, and coefficient of variation of 3.32E−08 m/s, 2.32E−08, and 69.86%, respectively.

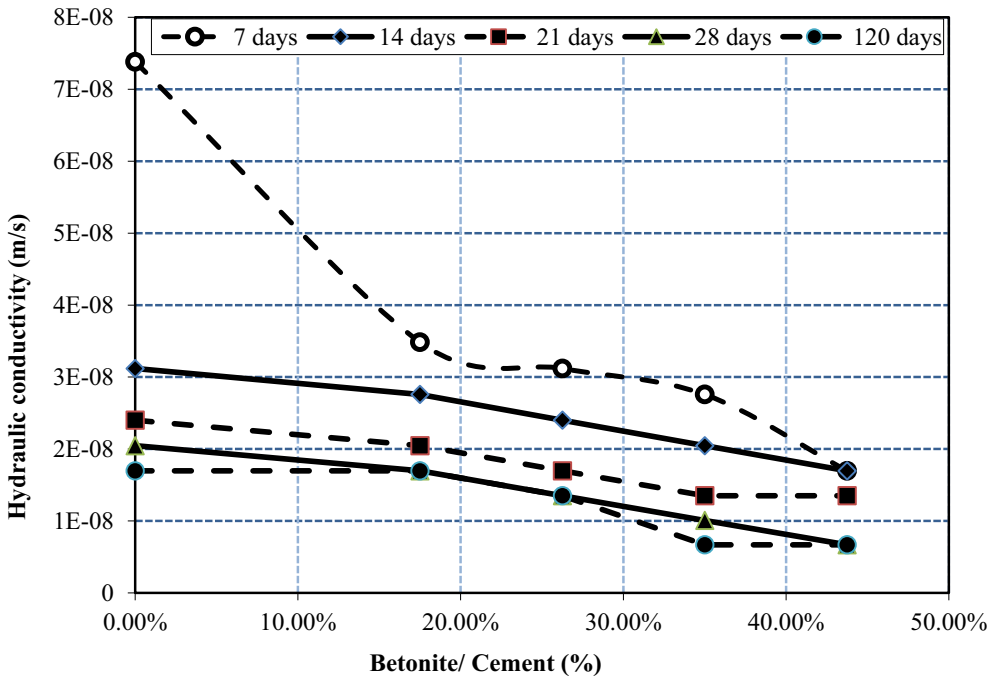

Fig. 11 Relationship between hydraulic conductivity and bentonite/cement ratio

On the other hand, the plastic concrete followed the same behavior of the control concrete as the testing age increased, and the hydraulic conductivity decreased. Results showed that the plastic concrete efficiently controlled the seepage of water with respect to the conventional concrete. The hydraulic conductivity for group II at 7, 14, 21, 28, and 120 days was 3.48E−08, 2.75E−08, 2.04E−08, 1.69E−08, and 1.69E−08 m/s, while their counterparts for group III were 3.11E−08, 2.40E−08, 1.69E−08, 1.35E−08, and 1.35E−08 m/s, respectively. Moreover, the hydraulic conductivity of groups IV and V was remarkably reduced compared to the other two plastic groups II and III. The hydraulic conductivity for group IV at 7, 14, 21, 28, and 120 days was 2.75E−08, 2.04E−08, 1.35E−08, 1.01E−08, and 6.68E−09 m/s, while their counterparts for group V were 1.69E−08, 1.69E−08, 1.35E−08, 6.68E−09, and 6.68E−09 m/s, respectively.

Based on the experimental relationships between the hydraulic conductivity and the bentonite/cement ratios at various ages depicted in Fig. 11, one can conclude that the hydraulic conductivity of plastic concrete mixes decreases with increasing compressive strength and increasing bentonite content within the plastic mixtures up to 28 days. There was obvious reduction in the hydraulic conductivity coefficient for plastic mixtures with bentonite reaching about 22% to 48% at age 7 days. It could be observed that the hydraulic conductivity of plastic mixtures at 28 and 120 days was approximately similar even if the testing age and the bentonite content were significantly varied. The average value of the hydraulic conductivity for mix I, II, III, IV, and V was 3.32E−08, 2.33E−08, 1.98E−08, 1.56E−08, and 1.21E−08, respectively.

Based on the experimental result shown in Fig. 11 and statistics analysis, the following linear correlations between hydraulic conductivity coefficients, the bentonite/cement ratios, and sample age were derived as follows:

$$K = \frac{1}{25t} - 2 \times 10^{-8} \frac{B}{C}, \tag{10}$$

where t is the sample age at test date in seconds.

Fig. 12 illustrates a comparison between the measured hydraulic conductivity coefficients values to the estimated values from the proposed equation (Eq. 10). This shows a very good relationship between calculated and measured values of the hydraulic conductivity coefficients as all the points are reasonably close to the equality line. This equation could be used to estimate the hydraulic conductivity coefficients.

4.7 Recorded Hydraulic Conductivity Versus Previous Analytical Equations.

This section presents a comparison between the experimentally recorded hydraulic conductivity and the previous analytical equations. It is important to

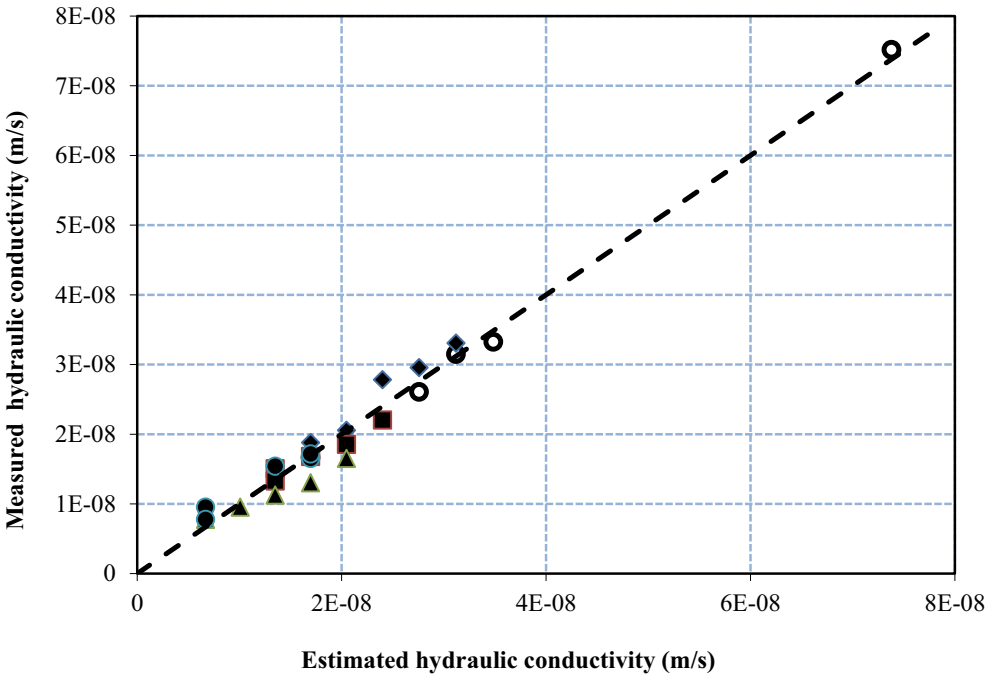

Fig. 12 Estimated versus measured hydraulic conductivity

Table 14 The experimental hydraulic conductivity results versus previous analytical model (m/s)

Experimental (EXP)	Analytical models (ANA)					
	Castro et al. (2009)	Kevern et al. (2009)	Neithalath et al. (2010)	Tho-in et al. (2012)	Bhutta et al. (2012)	Maguesvari and Narasimha (2013)
7.38E−08	0.85679775	19.76962279	4.80525E−10	0.046086	4.905606	0.329907601
3.11E−08	0.85679775	19.76962279	4.80525E−10	0.046086	4.905606	0.329907601
2.40E−08	0.8552569	19.71434527	3.83324E−10	0.0459583	4.91146	0.285400261
2.04E−08	0.85371882	19.65922231	3.05784E−10	0.0458309	4.917314	0.246897339
1.69E−08	0.85371882	19.65922231	3.05784E−10	0.0458309	4.917314	0.246897339
3.48E−08	0.8552569	19.71434527	3.83324E−10	0.0459583	4.91146	0.285400261
2.75E−08	0.8552569	19.71434527	3.83324E−10	0.0459583	4.91146	0.285400261
2.04E−08	0.85371882	19.65922231	3.05784E−10	0.0458309	4.917314	0.246897339
1.69E−08	0.85371882	19.65922231	3.05784E−10	0.0458309	4.917314	0.246897339
1.69E−08	0.85295082	19.63171866	2.73111E−10	0.0457673	4.920241	0.229639944
3.11E−08	0.85295082	19.63171866	2.73111E−10	0.0457673	4.920241	0.229639944
2.40E−08	0.85295082	19.63171866	2.73111E−10	0.0457673	4.920241	0.229639944
1.69E−08	0.85218351	19.60425348	2.4393E−10	0.0457038	4.923168	0.213588789
1.35E−08	0.85141689	19.57682673	2.17866E−10	0.0456404	4.926095	0.198659563
1.35E−08	0.85065096	19.54943835	1.94587E−10	0.0455771	4.929022	0.184773845
2.75E−08	0.85295082	19.63171866	2.73111E−10	0.0457673	4.920241	0.229639944
2.04E−08	0.85295082	19.63171866	2.73111E−10	0.0457673	4.920241	0.229639944
1.35E−08	0.85141689	19.57682673	2.17866E−10	0.0456404	4.926095	0.198659563
1.01E−08	0.85141689	19.57682673	2.17866E−10	0.0456404	4.926095	0.198659563
6.68E−09	0.85141689	19.57682673	2.17866E−10	0.0456404	4.926095	0.198659563
1.69E−08	0.85141689	19.57682673	2.17866E−10	0.0456404	4.926095	0.198659563
1.69E−08	0.85065096	19.54943835	1.94587E−10	0.0455771	4.929022	0.184773845
1.35E−08	0.85065096	19.54943835	1.94587E−10	0.0455771	4.929022	0.184773845
6.68E−09	0.84988572	19.52208828	1.73796E−10	0.0455139	4.931949	0.171858699

Table 15 The correlations between the experimental and theoretical hydraulic conductivity

	EXP /Castro et al	EXP/Kevern et al	EXP/Neithalath et al	EXP/Tho-in et al	EXP/Bhutta et al	EXP/ Maguesvari and Narasimha
Average	2.44E−08	1.06E−09	7.13E+01	4.54E−07	4.23E−09	8.59E−08
Standard deviation	1.6E−08	6.8E−10	25.4	2.9E−07	2.7E−09	3.8E−08
Coefficient of variation (%)	6.4E+01	6.4E+01	3.6E+01	6.4E+01	6.5E+01	4.4E+01
Maximum EXP/ANA	8.6E−08	3.7E−09	153.6	1.6E−06	1.5E−08	2.2E−07
Minimum EXP/ANA	7.8E−09	3.4E−10	30.7	1.5E−07	1.4E−09	3.4E−08

mention that the analytical hydraulic conductivity was calculated for every previous study based on the formulations described in Table 1. Table 14 lists the relationships between the experimental results and the analytical ones. The comparison's findings demonstrate that, with the exception of Neithalath et al.'s model, all hydraulic conductivity values calculated by the analytical models were higher than experimental records. The statistical results presented in Table 15 show that all analytical models were not able to successfully predict the experimental values of hydraulic conductivity. The average values between experimental results and analytical models were in the range of 1.06E−09–7.13E+01. Also standard deviation and coefficient of variation values indicate that all analytical models values were far from experimental ones. Inferring from this paragraph's comparison of experimental and analytical data on the hydraulic conductivity of plastic concrete, it is still urgently necessary to develop

mathematical equations that can accurately forecast these values, particularly when they vary over time.

5 Conclusion

Numerous laboratory tests were performed for various sand-bentonite-cement mixes, including the following: forty-five cylinders were used for the splitting tensile test; fifteen cylindrical specimens were used for the hydraulic conductivity and porosity tests; and a total of forty-five cubes were used for the compressive test. The main goal is to investigate changes in the mechanical and physical properties of secant pile material under various key parameters, such as water-to-cement ratio, bentonite-to-cement ratio, cement content, and sample age. The following conclusions can be made in light of the test results:

1) The hydraulic conductivity of both control and plastic concretes gradually decreased with the increase of the testing age. The hydraulic conductivity of control mixture at 7, 14, 21, 28, and 120 days was 7.38E−08, 3.11E−08, 2.40E−08, 2.04E−08, and 1.69E−08 m/s, respectively.
2) As the bentonite content increased, the hydraulic conductivity coefficient decreased. According to the experimental results, the average reduction in hydraulic conductivity for plastic concrete was in the range of 30%–64% compared to control concrete along the testing age of 120 days.
3) Based on compressive test results, the testing age has a significant effect on the compressive strength of the plastic concrete.
4) The reduction percentage in the compressive strength of plastic concrete samples with bentonite was in the range of 42–72%, 53–71%, 38–67%, 21–67%, and 17–64%, at 7, 14, 21, 28, and 120 days with respect to the control concrete (without bentonite).
5) The proposed formula to estimate the splitting tensile strength based on the compressive strength showed well agreement with the experimental records for samples of sand-bentonite-cement mixtures where standard deviation and coefficient of variation were 0.02, and 0.94%, respectively.
6) Based on the comparison between the experimental and analytical results of hydraulic conductivity of plastic concrete, it is still necessarily required to develop mathematical equations that can accurately predict the change of hydraulic conductivity with time.

Acknowledgements
The experimental tests were carried out by the material testing laboratory of the faculty of Engineering, Kafrelsheikh University, Egypt.

Author contributions
AB contributed to conceptualization, methodology, idea of the research, writing, and writing––review and editing. WM was involved in conceptualization, methodology, idea of the research, writing, and writing––review, supervision, and editing. All authors read and approved the final manuscript.

Authors' information
Ali Basha, Associate Professor, Civil Engineering Department, Faculty of Engineering, Kafrelsheikh University, Kafrelsheikh, 33511, Egypt. Walid Mansour, Assistant Professor, Civil Engineering Department, Faculty of Engineering, Kafrelsheikh University, Kafrelsheikh, 33511, Egypt.

Funding
Open access funding provided by The Science, Technology & Innovation Funding Authority (STDF) in cooperation with The Egyptian Knowledge Bank (EKB). The authors received no financial support for the research, authorship, and/or publication of this article.

Availability of data and materials
Some of all the data, models, or code that support the findings of this study are available from the corresponding author upon reasonable request.

Declarations

Ethics approval and consent to participate
None.

Consent for publication
None.

Competing interests
No potential conflict of interest was reported by the authors.

Received: 21 October 2022 Accepted: 4 February 2023
Published online: 01 May 2023

References

Alós Shepherd, D., Kotan, E., & Dehn, F. (2020). Plastic concrete for cut-off walls: A review. *Construction and Building Materials., 255*, 119248.
ASTM-C496. Splitting tensile strength of cylindrical concrete", West Conshohocken, PA 1996.
Bagheri, A. R., Alibabaie, M., & Babaie, M. (2008). Reduction in the permeability of plastic concrete for cut-off walls through utilization of silica fume. *Construction and Building Materials, 22*(6), 1247–1252.
Barnhouse, P. W., & Srubar, W. V. (2016). Material characterization and hydraulic conductivity modeling of macroporous recycled-aggregate pervious concrete. *Construction and Building Materials, 110*, 89–97. https://doi.org/10.1016/j.conbuildmat.2016.02.014
Bhutta, M. A. R., Tsuruta, K., Mirza, J., Tho-in, T., Sata, V., Chindaprasirt, P., & Jaturapitakkul, C. (2012). Evaluation of high-performance porous concrete properties. *Construction and Building Materials, 31*, 67–73. https://doi.org/10.1016/j.conbuildmat.2011.12.024
Castro, J., De Solminihac, H., Videla, C., & Fernández, B. (2009). Estudio de dosificaciones en laboratorio para pavimentos porosos de hormigón. *Revista Ingeniería De Construcción, 24*(3), 271–284. https://doi.org/10.4067/S0718-50732009000300005
Chandrappa, A. K., & Biligiri, K. P. (2016). Comprehensive investigation of permeability characteristics of pervious concrete: A hydrodynamic approach. *Construction and Building Materials, 123*, 627–637. https://doi.org/10.1016/j.conbuildmat.2016.07.035

ECP 203. Housing and Building National Research Center, Egyptian Code for Designing and Constructing Reinforced Concrete Structures, Cairo, Egypt 2017.
El-Nimr, M. T., Basha, A. M., Abo-Raya, M. M., & Zakaria, M. H. (2022). General deformation behavior of deep excavation support systems: A review. *Global Journal of Engineering and Technology Advances., 10*(01), 039–057. https://doi.org/10.30574/gjeta.2022.10.1.0181
Fadaie, M. A., Nekooei, M., & Javadi, P. (2019). Effect of dry and saturated bentonite on plastic concrete. *KSCE Journal of Civil Engineering*. https://doi.org/10.1007/s12205-019-0835-2
Flessati, L., Della Vecchia, G., & Musso, G. (2021). Mechanical behavior and constitutive modeling of cement-bentonite mixtures for cutoff walls. *Journal of Materials in Civil Engineering, 33*(3), 04020483. https://doi.org/10.1061/(asce)mt.1943-5533.0003584
Gao, D. Y., Yan, K. B., Hu, L. M., & Song, S. Q. (2009). Influence of bentonite types on the properties of plastic concrete. *J. Hydro. Eng., 28*(3), 112–116.
Guo, X. M., & Zhu, W. B. (2008). The mix proportion of plastic concrete and its characteristics and application to cut-off wall of embankment dam. *J. Changsha Univ. Sci. Tech., 5*(3), 41–46.
Hinchberger, S., Weck, J., & Newson, T. (2010). Mechanical and hydraulic characterization of plastic concrete for seepage cut-off walls. *Canadian Geotechnical Journal, 47*(4), 461–471.
Huang, B., Wu, H., Shu, X., & Burdette, E. G. (2010). Laboratory evaluation of permeability and strength of polymer-modified pervious concrete. *Construction and Building Materials, 24*, 818–823. https://doi.org/10.1016/j.conbuildmat.2009.10.025
Ibrahim, A., Mahmoud, E., Yamin, M., & Patibandla, V. C. (2014). Experimental study on Portland cement pervious concrete mechanical and hydrological properties. *Construction and Building Materials, 50*, 524–529. https://doi.org/10.1016/j.conbuildmat.2013.09.022
Iravanian, A., & Bilsel, H. (2016). Tensile strength properties of sand-bentonite mixtures enhanced with cement. *Procedia Engineering, 143*, 111–118. https://doi.org/10.1016/j.proeng.2016.06.015
Kevern JT, Schaefer VR, Wang K. 2009. Predicting performance of pervious concrete using fresh unit Weight, in: NRMCA Concrete Technology Forum: focus on performance prediction
Liu, J. P., Li, L., Miao, C. W., Tian, Q., Ran, Q. P., & Wang, Y. J. (2011). Reduction of water evaporation and cracks on plastic concrete surface by monolayers. *Colloids and Surfaces a: Physicochemical and Engineering Aspects, 384*(1–3), 496–500.
Maguesvari, M. U., & Narasimha, V. L. (2013). Studies on characterization of pervious concrete for pavement applications. *Procedia-Social and Behavioral Sciences, 104*, 198–207. https://doi.org/10.1016/j.sbspro.2013.11.112
Mansour, W., & Fayed, S. (2021). Flexural rigidity and ductility of RC beams reinforced with steel and recycled plastic fibers. *Steel and Composite Structures, 41*, 317–334.
Mansour, W., Tayeh, B. A., & Tam, L. H. (2022). Finite element analysis of shear performance of UHPFRC-encased steel composite beams: Parametric study. *Engineering Structures, 271*, 114940.
Neithalath, N., Sumanasooriya, M. S., & Deo, O. (2010). Characterizing pore volume, sizes, and connectivity in pervious concretes for permeability prediction. *Materials Characterization, 61*, 802–813. https://doi.org/10.1016/j.matchar.2010.05.004
Park, S. B., & Tia, M. (2004). An experimental study on the water-purification properties of porous concrete. *Cement and Concrete Research, 34*(2), 177–184. https://doi.org/10.1016/s0008-8846(03)00223-0
Royal, A. C. D., Opukumo, A. W., Qadr, C. S., Perkins, L. M., & Walenna, M. A. (2017). Deformation and compression behaviour of a cement-bentonite slurry for groundwater control applications. *Geotechnical and Geological Engineering*. https://doi.org/10.1007/s10706-017-0359-9
Sakr, M. A., Sleemah, A. A., Khalifa, T. M., & Mansour, W. N. (2018). Behavior of RC beams strengthened in shear with ultra-high performance fiber reinforced concrete (UHPFRC). *MATEC Web of Conferences, 199*, 09002. https://doi.org/10.1051/matecconf/201819909002
Sandoval, G. F. B., Galobardes, I., De Moura, A. C., & Toralles, B. M. (2020). Hydraulic behavior variation of pervious concrete due to clogging. *Case Studies in Construction Materials., 13*, e00354. https://doi.org/10.1016/j.cscm.2020.e00354
Sandoval, G. F. B., Galobardes, I., Teixeira, R. S., & Toralles, B. M. (2017). Comparison between the falling head and the constant head permeability tests to assess the permeability coefficient of sustainable Pervious Concretes. *Case Studies in Construction Materials, 7*, 317–328. https://doi.org/10.1016/j.cscm.2017.09.001
Tho-in, T., Sata, V., Chindaprasirt, P., & Jaturapitakkul, C. (2012). Pervious high-calcium fly ash geopolymer concrete. *Construction and Building Materials, 30*, 366–371. https://doi.org/10.1016/j.conbuildmat.2011.12.028
Wang, S. W., Yu, H. C., Gao, D. Y., & Zhao, L. M. (2011). Testing on elastic modulus of plastic concrete. *Hydro. Eng. Geol., 38*(3), 73–76.
Wu, H., Liu, Z., Sun, B., Yin, J., Chandrappa, A. K., & Biligiri, K. P. (2016). Experimental investigation on freeze-thaw durability of Portland cement pervious concrete (PCPC). *Construction and Building Materials, 117*, 63–71. https://doi.org/10.1016/j.conbuildmat.2016.04.130
Xiong, H., Wang, Q. Y., Gao, X. Z., Zhou, W. P., & Gao, M. J. (2011). Stress deformation analysis of plastic concrete cutoff wall for the first stage cofferdam of Shawan hydropower station. *Journal of Hydroelectric Engineering, 29*(2), 197–203.
Xu, H., Zhu, W., Qian, X., Wang, S., & Fan, X. (2016). Studies on hydraulic conductivity and compressibility of backfills for soil-bentonite cutoff walls. *Applied Clay Science, 132*, 326–335. https://doi.org/10.1016/j.clay.2016.06.025
Zhang, P., Guan, Q., & Li, Q. (2013). Mechanical properties of plastic concrete containing bentonite. *Research Journal of Applied Sciences, Engineering and Technology, 5*(4), 1317–1322.
Ziccarelli, M., & Valore, C. (2018). Hydraulic conductivity and strength of pervious concrete for deep trench drains. *Geomechanics for Energy and the Environment*. https://doi.org/10.1016/j.gete.2018.09.001

Publisher's Note